

B Side Electron Transfer in a *Rhodobacter sphaeroides* Reaction Center Mutant in Which the B Side Monomer Bacteriochlorophyll Is Replaced with Bacteriopheophytin: Low-Temperature Study and Energetics of Charge-Separated States

Evaldas Katilius,* Zivile Katiliene, Su Lin, Aileen K. W. Taguchi, and Neal W. Woodbury

Department of Chemistry and Biochemistry and the Center for the Study of Early Events in Photosynthesis, Arizona State University, Tempe, Arizona 85287-1604

Received: August 24, 2001

The mutation, HL(M182), in the *Rhodobacter sphaeroides* reaction center (RC) results in the replacement of the monomer bacteriochlorophyll (BChl) on the inactive side (B side) of the RC with a bacteriopheophytin (BPheo; the new cofactor is referred to as ϕ_B). In ϕ_B -containing RCs, the first excited state of the primary donor (P^*) decays with an accelerated time constant of 2.6 ± 0.1 ps at room temperature as compared to 3.1 ± 0.2 ps in wild-type (WT) RCs. At low temperatures, P^* decay is essentially the same in the HL(M182) mutant and WT RCs: 1.4 ± 0.1 ps at 77 K and 1.1 ± 0.1 ps at 9 K. The yield of the charge-separated $P^+\phi_B^-$ state decreases from 35% at room temperature to 12% at 77 and 9 K. The decreased $P^+\phi_B^-$ yield is apparently due to the fact that the rate of the charge separation along the A side of the RC at low temperature increases, while the rate along the B side remains essentially unchanged. From measurements of the long-lived fluorescence decay at room temperature, the standard free energy of the $P^+\phi_B^-$ state is estimated to be about 0.16 ± 0.04 eV below P^* . Given a difference between the midpoint potentials of BChl and BPheo of 0.26 ± 0.03 V, the standard free energy of the $P^+B_B^-$ state in WT RC is estimated to be 0.1 ± 0.07 eV above P^* .

Introduction

In bacterial photosynthesis, light energy is absorbed by antenna complexes and transferred to the reaction center (RC), where it drives transmembrane charge separation. The structure and function of photosynthetic RCs from purple nonsulfur photosynthetic bacteria such as *Rhodobacter (Rb.) sphaeroides* have been extensively studied.^{1–3} The RC consists of three protein subunits L, M, and H, which bind 10 cofactors: four bacteriochlorophylls (BChl), two bacteriopheophytins (BPheo), two quinone molecules, a carotenoid molecule, and a nonheme iron. BChl, BPheo, and quinone cofactors are arranged in nearly symmetric branches, and thus, there are two potential pathways for photosynthetic electron transfer (usually labeled A and B). The two potential electron transfer pathways both start with a primary donor (P; a pair of BChl), followed by a monomer bacteriochlorophyll (either B_A or B_B), a bacteriopheophytin (either H_A or H_B), and then a ubiquinone (either Q_A or Q_B). However, upon excitation of P in wild-type (WT) RCs, the initial electron transfer occurs almost exclusively along the cofactors on the A side.^{4,5} Apparently, an electron is transferred from the first excited state of P (P^*) to B_A in about 3.5 ps and then to H_A in less than a picosecond at room temperature.^{6,7} Subsequently, the electron is transferred to the primary quinone acceptor, Q_A , in about 200 ps and then to the secondary quinone acceptor, Q_B , in about 200 μ s. The quantum yield of this process is near unity.⁸

Most estimates reported in the literature for the electron transfer ratio along the A side vs the B side in WT RCs are in the range of 30:1–200:1 favoring the A side.^{4,9–11} From the RC crystal structure, it is clear that the approximate symmetry

of the RC breaks down at the level of the specific amino acids that make up the environment of the A and B cofactors. Therefore, mutagenesis has been a powerful tool in the study of electron transfer directionality. These studies have involved both mutants that alter the environment of the cofactors and mutants that result in changes in the chemical identity of the cofactors themselves.^{12–20}

A great deal has been learned by studying B side electron transfer in mutants that have the primary electron acceptor H_A replaced with the bacteriochlorophyll making it possible to see small changes in the Q_X transition region (around 530 nm) of H_B . By adding the mutations which modify the environment of H_A , B_A , and B_B in such a way that electron transfer along the A side is greatly slowed and electron transfer along the B side is sped up, charge separation resulting in the $P^+H_B^-$ state with a quantum yield of up to 23% has been observed.^{17,19,20} Also, the addition of mutations, which remove the Q_A from its binding pocket, has made it possible to observe electron transfer from H_B to Q_B .²¹

Another approach to promoting B side electron transfer is to greatly stabilize the initial charge-separated state without altering the A side cofactors. Almost 40% B side electron transfer is observed in HL(M182), a mutant in which B_B has been replaced with a BPheo, making it much easier to reduce.¹⁸ In this case, electron transfer along the B side occurs with a rate comparable to that on the A side in WT RCs, suggesting that it is really the relative standard free energy of $P^+B_A^-$ and $P^+B_B^-$ with respect to P^* , rather than coupling between cofactors, that controls the direction of electron transfer. Unfortunately, there is still considerable uncertainty in the standard free energy values for those states. While the standard free energy of $P^+B_A^-$ is believed to be in the range of 50–100 meV below P^* ,^{20,22–24} the energy of the $P^+B_B^-$ state was estimated from theoretical calculations

* Author to whom correspondence should be addressed. Fax: (480)-965-2747. E-mail: Evaldas@asu.edu.

to be at least 0.1 eV above P^* .²⁵ The standard free energy of the $P^+H_B^-$ state is slightly lower than that of P^* as estimated from the theoretical calculations²⁵ and supported by the experimental observation of that state.^{17,19,20,26} However, we have previously shown that in the HL(M182) mutant, electron transfer only proceeds from the P^* to the $P^+\phi_B^-$ state and does not continue on to $P^+H_B^-$, suggesting that the standard free energy of $P^+\phi_B^-$ is below that of $P^+H_B^-$ in this mutant.¹⁸

In this paper, effects of energetics are investigated by further considering the properties of the HL(M182) mutant at room and low (cryogenic) temperatures. The results allow the estimation of the standard free energy of the $P^+\phi_B^-$ state in the mutant, and this in turn allows the estimation of the relative standard free energy of $P^+B_B^-$ in the WT RC.

Experimental Section

The construction of the HL(M182) mutation and the isolation of RCs have been described previously.¹⁸ All results were also obtained with samples that have a polyhistidine (poly-His) tag.²⁷ WT RCs with poly-His tags were isolated as previously described²⁷ with the following modifications. To improve the specific binding of the solubilized RCs to the Ni-NTA column, 5 mM imidazole and 150 mM NaCl were added to the solution before loading it onto the Ni-NTA column as well as to the washing buffer. This improved the specific binding of the poly-His-tagged RCs to the column and resulted in faster purification of the RCs. However, in the case of the HL(M182) mutant RCs, the addition of imidazole during washing of the column resulted in a variable BChl to BPheo pigment ratio of the RCs, while omission of the imidazole during washing usually yielded samples with a pigment ratio (molar ratio of BChl to BPheo) of approximately 1, as would be expected for the exchange of one BChl with a BPheo in the RC. The change of the pigment ratio in the presence of imidazole is most probably due to the ability of the imidazole to ligate the Mg atom in BChl as shown in vitro.²⁸ Therefore, imidazole was omitted from the washing buffer during isolation of the mutant, and the RC elution from the Ni-NTA column was performed with a buffer containing 50 mM ethylenediaminetetraacetic acid instead of 50 mM imidazole. RCs were then dialyzed overnight and additionally purified via chromatography on a (diethylamino)ethyl column.²⁹ This altered procedure yielded samples of the poly-His-tagged HL(M182) mutant with the same pigment ratio as measured in the isolated HL(M182) mutant RCs without the poly-His tag.

For low-temperature (9 and 77 K) absorbance and transient absorbance measurements, samples were cooled using a closed circulated helium displex (APD) or Optistat DN cryostat (Oxford Instruments). Sample preparation was performed as described previously.²⁶ The femtosecond transient absorbance apparatus has also been described previously.¹⁸ The fluorescence kinetics were measured using a time-correlated single photon counting system.^{30,31} Samples with prerduced Q_A were excited with vertically polarized light at 860 nm from a Ti-sapphire laser (Spectra Physics Tsunami, <2 ps pulses at 4 Mz repetition rate using a Pulse Selector, model 3980). Fluorescence was filtered through a polarizer at the magic angle relative to the vertical polarization of the excitation pulse and a monochromator with a spectral bandwidth of 16 nm. Kinetics were measured at 890 nm and fitted to a sum of exponential decays using a data analysis program written with MATLAB software (Mathworks, Inc.). The standard free energies of the $P^+H_A^-$ and $P^+\phi_B^-$ states were estimated from the fluorescence as described previously.^{31–33}

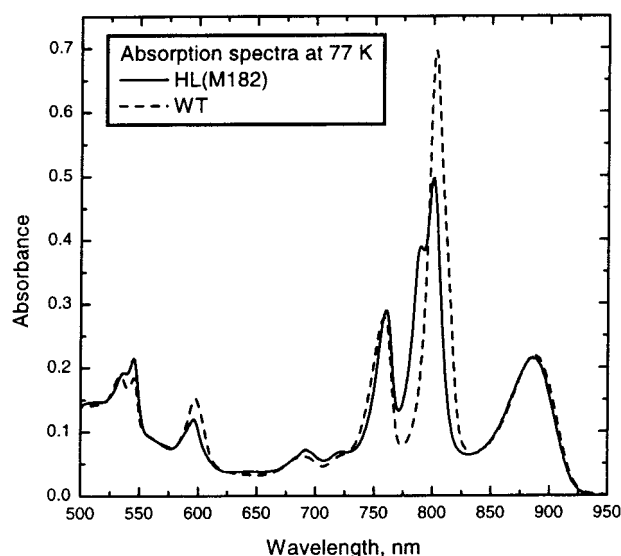


Figure 1. Ground state absorption spectra of HL(M182) mutant (solid line) and WT (dashed line) RCs at 77 K. The spectra were normalized at the maximum of the P band (885 nm).

Results

The ground state absorption spectra of the HL(M182) mutant and WT RCs at 77 K are shown in Figure 1. As previously described, the replacement of B_B with ϕ_B causes the spectral features usually associated with the B_B molecule to disappear and new spectral features associated with the exchanged bacteriopheophytin molecule to appear. At low temperatures, these changes are even more pronounced than at room temperature. As shown in Figure 1, the B absorption band near 800 nm has been significantly altered. The long wavelength side of the band, which is usually associated with B_B absorption, has disappeared, and a new band with a maximum at 790 nm has become visible. As seen at room temperature, the absorption of the Q_X band of the BChl molecules near 600 nm decreases, and there is an increase in the absorption of the BPheo Q_X band at 545 nm. The absorption of the exchanged pigment ϕ_B shifts from 540 nm at room temperature to 545 nm at 77 K and overlaps the absorption of the H_A band at 545 nm.

Transient absorption measurements of the HL(M182) mutant RCs at room temperature showed that the P^* -stimulated emission decay is faster than in WT RCs: 2.6 ± 0.1 and 3.1 ± 0.2 ps for HL(M182) and WT RCs, respectively.¹⁸ At low temperatures, the P^* stimulated emission decays observed for HL(M182) and the WT are indistinguishable within our experimental time resolution: about 1.3 ± 0.1 ps at 77 K and 1.1 ± 0.1 ps at 9 K for both samples. Apparently, the increase of the A side electron transfer rate at low temperatures is not accompanied by an increase in the rate of B side electron transfer in the mutant. Therefore, the overall P^* decay kinetics in the HL(M182) mutant at low temperature is dominated by the A side electron transfer.

The transient absorption kinetics of HL(M182) RCs measured on a 1 ns time scale at low temperature resembles the kinetics at room temperature. Most of the RCs in the sample decay with a time constant of many nanoseconds ($P^+H_A^-$ decays with a roughly 15 ns lifetime), and a decay-associated spectrum for the long-lived kinetic component corresponds to $P^+H_A^-$ (Figure 2).^{4,5} A small fraction of the RCs give rise to a distinct kinetic decay component with a P band bleaching near 885 nm and bleaching of the new ground state band at 785 nm that recover with a lifetime of approximately 190 ± 10 ps at both 77 and 9

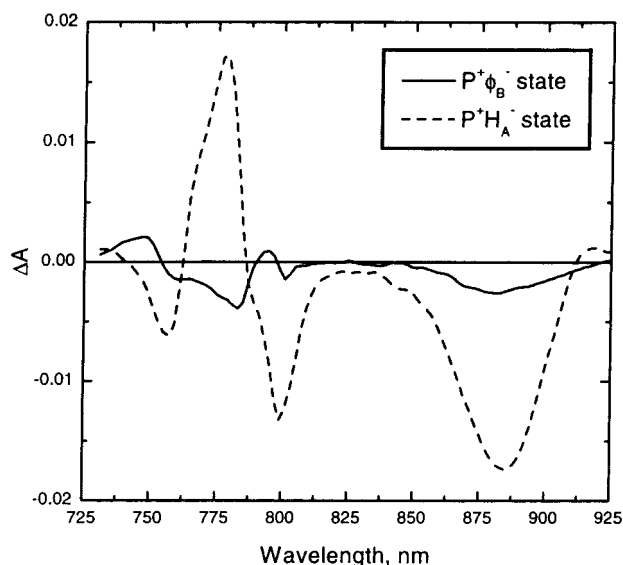


Figure 2. Decay-associated spectra corresponding to the $P^+\phi_B^-$ (solid line) and $P^+H_A^-$ (dashed line) states. The spectra of the long-lived and 190 ps decay components were obtained from global fitting of the time-resolved absorbance change spectra of HL(M182) RCs with one exponential term and a constant. The fits were performed on data taken over a 1 ns time scale.

K. This 190 ps decay component is very similar in both its spectral features and its lifetime to the $P^+\phi_B^-$ recombination component observed at room temperature.¹⁸ The yield of the $P^+\phi_B^-$ state at low temperatures can be estimated from the relative ratio of the bleaching of the ground state P band at 880 nm in the two decay-associated spectra. The yield of $P^+\phi_B^-$ at low temperature is less than that at room temperature; at both 77 and 9 K, it is 12%.

At low temperatures, the H_A and H_B absorption bands are well-separated (see the WT spectrum in Figure 1), making it possible to follow the charge separation along the A or B side at the level of the BPheo molecules in WT RCs.^{17,19,20,26} However, the absorption of ϕ_B in the Q_X region overlaps the H_A absorption band at 545 nm (see above and Figure 1), making it impossible to distinguish between electron transfer to H_A vs ϕ_B . Thus, a detailed analysis of the time-resolved spectra in the Q_X region is not presented here.

Time-correlated single photon counting was used to measure the fluorescence kinetics from quinone-reduced WT and HL(M182) mutant RCs at room temperature. In both cases, four exponential decay components are required to achieve the best fit on statistical grounds (reduced χ^2 between 1.0 and 1.15, see Table 1). For both the WT and HL(M182), the prompt fluorescence decay time is limited by the instrument response function; therefore, the lifetimes of the prompt components were fixed at the values acquired from the transient absorption results.¹⁸ Particular attention was paid to the kinetics within the first nanosecond after excitation. As was shown previously using transient absorption measurements, the $P^+\phi_B^-$ state recombines in about 200 ps at room temperature.¹⁸ Therefore, one would expect to observe a fluorescence decay component corresponding to the charge recombination of this state (reforming P^*) in the fluorescence kinetics, as observed previously for subnanosecond and nanosecond fluorescence decay components due to $P^+H_A^-$ recombination in WT RCs.^{31–34} As one can see from Table 1, for the HL(M182) mutant, a fluorescence lifetime of 240 ps was determined, which corresponds well to the observed 200 ps lifetime from transient absorption data.¹⁸ However, the WT also shows a subnanosecond component on this time scale,

and the difference in the initial amplitudes of the mutant and WT components is quite small (the WT value is about 10% smaller than that of the mutant). This indicates that the recombination of the $P^+\phi_B^-$ state causes only a small perturbation in the long-lived fluorescence amplitude as compared to the fluorescence in WT RCs. For this reason, it will only be possible to use this method to set limits on the energetics of $P^+\phi_B^-$ (see Discussion).

Discussion

Excitation of the *Rb. sphaeroides* HL(M182) mutant RCs at room temperature gives rise to electron transfer on the B side of the RC, forming the $P^+\phi_B^-$ state with a yield of $35 \pm 5\%$.¹⁸ However, at low temperatures, the yield of the B side electron transfer forming $P^+\phi_B^-$ is decreased substantially. This is most likely due to the 3-fold increase in the rate of the electron transfer along the A side with decreasing temperature. The decrease in the yield from 35% at room temperature to 12% at 9 K corresponds to the decrease of the A side electron transfer lifetime from 3.5 to 1.1 ps, indicating that the rate constant for the electron transfer from P^* to $P^+\phi_B^-$ does not speed up with decreasing temperature as does the A side rate constant. Taking into account the yield of the $P^+\phi_B^-$ state, one can estimate the rate constant (or lifetime) for charge separation along the B side. Considering the observed rate constant for P^* decay at the three temperatures and the observed quantum yield of $P^+\phi_B^-$, one can calculate that the B side electron transfer rate from P^* to $P^+\phi_B^-$ remains roughly constant between room temperature and 9 K with a time constant between 7 and 9 ps. The estimated lifetime is about an order of magnitude longer than the lifetime of the A side electron transfer at low temperature, explaining the similarity of the P^* decay times in the WT and HL(M182) under these conditions.

Similarly, the charge recombination rate of $P^+\phi_B^-$ to the ground state is essentially temperature-independent (both the room temperature value measured previously¹⁸ and the one reported here at low temperature are about 200 ps). Therefore, there are apparently no activation barriers to either process.

It is possible to determine the standard free energy change between P^* and subsequent charge-separated states by monitoring the long-lived fluorescence due to recombination of charge separation when further electron transfer is blocked.^{31–35} These measurements are based on the idea that the initial amplitude of the long-lived fluorescence represents the equilibrium population of P^* immediately after charge separation. From this, an equilibrium constant and thus a standard free energy for the charge separation reaction can be calculated.

A lower limit for the standard free energy gap between $P^+\phi_B^-$ and P^* can be obtained by assuming that the 240 ps fluorescent decay component is all due to the delayed fluorescence from $P^+\phi_B^-$ recombination. In this case, the energy of $P^+\phi_B^-$ is estimated to be about 0.13 eV below P^* . However, as mentioned above, WT also shows a component with about a 160 ps lifetime and a very similar amplitude to the 240 ps component observed for HL(M182) RCs. A more conservative value of the $P^+\phi_B^-$ free energy could be estimated by assuming that the amplitude of fluorescence due to $P^+\phi_B^-$ recombination is simply the difference between the amplitudes of the 160 ps component in the WT and the 240 ps component in HL(M182). In this case, the standard free energy of the $P^+\phi_B^-$ state would be about 0.2 eV below P^* . Taking into account these limits, we estimate that the energy of the $P^+\phi_B^-$ state is in the range of 0.16 ± 0.04 eV below P^* . Note that the upper end of this range, which depends on the use of the whole initial amplitude of the 240 ps

TABLE 1: Fluorescence Kinetics of WT and HL(M182) RCs at Room Temperature

sample	τ_1 (ps) ^a	A ₁ (%)	τ_2 (ps)	A ₂ (%)	τ_3 (ns)	A ₃ (%)	τ_4 (ns)	A ₄ (%)	χ^2
HL(M182)	2.6	99.2798	240	0.5165	1.22	0.1355	6.41	0.0681	1.09
WT	3.5	99.3459	170	0.4706	1	0.1225	6.15	0.061	1.14

^a The presented lifetimes and the amplitudes are the fitting results of the kinetics measured at 890 nm. The amplitudes were normalized to 100%. The lifetimes of the first components for both samples were fixed, as the time resolution of the instrument does not allow their accurate determination.

component is quite well-defined, while the estimation of the lower end of the range is more tentative. However, the lower boundary will be considered in more detail below.

Given the relative standard free energy of $P^+\phi_B^-$, it is possible to estimate the relative standard free energy of the $P^+B_B^-$ state. As determined in vitro in various solvents, the midpoint potential for the BPheo/BPheo⁻ redox couple is about 230–300 mV more positive than that of BChl/BChl⁻ couple.^{36,37} Therefore, if one assumes that the difference between the BChl and the BPheo midpoint potentials is about the same in the B_B binding site as it is in vitro, the $P^+B_B^-$ state can be estimated to be 0.1 ± 0.07 eV above P^* . Given that the standard free energy of the $P^+B_A^-$ state has been estimated to be about 50 meV below P^* in *Rb. sphaeroides*^{22–24} or even 100 meV below P^* in *Rb. capsulatus*,²⁰ this estimate of the $P^+B_B^-$ relative standard free energy is consistent with the fact that B side electron transfer is much slower than A side electron transfer in WT RCs at room temperature. The estimate of the $P^+B_B^-$ relative standard free energy is also consistent with the fact that $P^+B_B^-$ is close enough in free energy to P^* so that relatively minor changes in the electrostatic environment can make electron transfer along the B side possible.^{17,19,20} In addition, previous theoretical calculations have suggested that the $P^+B_B^-$ state is 0.24 ± 0.13 eV higher than P^* ,²⁵ which is also in reasonable agreement with our results. As mentioned above, the lower limit estimated above for the $P^+\phi_B^-$ relative standard free energy is less well-defined than the upper limit. However, if it was significantly lower than 0.2 eV below P^* , that would bring the value for the relative standard free energy of $P^+B_B^-$ down nearly to the level of P^* , which seems unreasonable, taking into account the strong directionality of electron transfer in WT RC.

As previously reported, the electron transfer on the B side does not continue on from $P^+\phi_B^-$ to $P^+H_B^-$ in the HL(M182) mutant.¹⁸ Other mutants that enhance B side electron transfer have resulted in electron transfer from P to H_B and even to Q_B.^{17,19–21} Also, multiphoton excitation of R-26 RCs results in roughly 30% electron transfer along the B side as far as H_B.²⁶ The lack of electron transfer past $P^+\phi_B^-$ in the ϕ_B mutant is therefore almost certainly due to the relative energetics of the $P^+\phi_B^-$ and $P^+H_B^-$ states. The relative standard free energy of the $P^+H_B^-$ state has not previously been determined experimentally, although theoretical calculations place it about 0.07 eV below P^* .²⁵ Thus, the theoretical value for the relative standard free energy of $P^+H_B^-$ is consistent with our estimate of the relative standard free energy of the $P^+\phi_B^-$ state (0.16 ± 0.04 eV below P^*). To investigate the relative energetics of $P^+\phi_B^-$ and $P^+H_B^-$ further, additional mutations placing an aspartic or glutamic acid near the exchanged pigment ϕ_B (which presumably should raise the relative free energy of the $P^+\phi_B^-$ state closer to P^*)²⁰ are being characterized.

Previously, theoretical calculations of the electronic matrix elements between the primary donor P and the monomer BChl on the A and B sides suggest that the unidirectionality of the charge separation in the *Rb. sphaeroides* RC is strongly dependent on the difference in the electronic coupling in the two branches.^{38,39} The electronic matrix element on the B side was calculated to be about 30 times smaller than on the A side;

thus, the coupling on the B side would be almost 3 orders of magnitude smaller than on the A side. The authors argued that this difference is one of the main reasons for the unidirectional electron transfer.³⁹ However, the results presented above and previously¹⁸ for electron transfer forming the $P^+\phi_B^-$ state imply that the coupling on the B side cannot be drastically different from that on the A side. In fact, assuming that the BChl to BPheo conversion did not radically alter the coupling with P, the calculated 2–3-fold difference in A vs B side matrix elements in RCs from *Rhodospseudomonas viridis* (see ref 39 and references therein) is more in line with our results. Given the relatively high rate of B side electron transfer in the ϕ_B mutant, at both room temperature and low temperature, it seems more likely that the relative energetics of the $P^+B_A^-$ and $P^+B_B^-$ states is the dominant factor in determining electron transfer directionality.

Acknowledgment. This research was supported by NSF Grant MCB9817388. The transient spectrometer used was funded by the NSF Grant BIR9512970. This publication is No. 501 from The Center for the Study of Early Events in Photosynthesis. We thank Prof. S. Boxer for providing us with the *Rb. sphaeroides* strains containing poly-His-tagged WT and HL(M182) RC genes.

References and Notes

- (1) Hoff, A. J.; Deisenhofer, J. *Phys. Rep.* **1997**, 287, 1–247.
- (2) Parson, W. W. Photosynthetic bacterial reaction centres. In *Protein Electron Transfer*; Bendall, S. D., Ed.; BIOS Scientific Publishers: Oxford, 1996; pp 125–160.
- (3) Woodbury, N. W.; Allen, J. P. The pathway, kinetics and thermodynamics of electron transfer in wild type and mutant reaction centers of purple nonsulfur bacteria. In *Anoxygenic Photosynthetic Bacteria*; Blankenship, R. E., Madigan, M. T., Bauer, C. E., Eds.; Kluwer Academic Publishers: Dordrecht, 1995; Vol. 2, pp 527–557.
- (4) Kirmaier, C.; Holten, D.; Parson, W. W. *Biochim. Biophys. Acta* **1985**, 810, 49–61.
- (5) Kirmaier, C.; Holten, D.; Parson, W. W. *Biochim. Biophys. Acta* **1985**, 810, 33–48.
- (6) Holzappel, W.; Finkle, U.; Kaiser, W.; Oesterheld, D.; Scheer, H.; Stiltz, H. U.; Zinth, W. *Chem. Phys. Lett.* **1989**, 160, 1–7.
- (7) Sporlein, S.; Zinth, W.; Meyer, M.; Scheer, H.; Wachtveitl, J. *Chem. Phys. Lett.* **2000**, 322, 454–464.
- (8) Wraight, C. A.; Clayton, R. K. *Biochim. Biophys. Acta* **1973**, 333, 246–260.
- (9) Kellogg, E. C.; Kolaczowski, S.; Wasielewski, M. R.; Tiede, D. M. *Photosynth. Res.* **1989**, 22, 47–59.
- (10) Michel-Beyerle, M. E.; Plato, M.; Deisenhofer, J.; Michel, H.; Bixon, M.; Jortner, J. *Biochim. Biophys. Acta* **1988**, 932, 52–70.
- (11) Tiede, D. M.; Kellogg, E.; Breton, J. *Biochim. Biophys. Acta* **1987**, 892, 294–302.
- (12) Taguchi, A. K. W.; Stocker, J. W.; Alden, R. G.; Causgrove, T. P.; Peloquin, J. M.; Boxer, S. G.; Woodbury, N. W. *Biochemistry* **1992**, 31, 10345–10355.
- (13) Stocker, J. W.; Taguchi, A. K. W.; Murchison, H. A.; Woodbury, N. W.; Boxer, S. G. *Biochemistry* **1992**, 31, 10356–10362.
- (14) McDowell, L. M.; Gaul, D.; Kirmaier, C.; Holten, D.; Schenck, C. C. *Biochemistry* **1991**, 30, 8315–8322.
- (15) Kirmaier, C.; Gaul, D.; DeBey, R.; Holten, D.; Schenck, C. C. *Science* **1991**, 251, 922–927.
- (16) Robles, S. J.; Breton, J.; Youvan, D. C. *Science* **1990**, 248, 1402–1405.
- (17) Heller, B. A.; Holten, D.; Kirmaier, C. *Science* **1995**, 269, 940–945.

- (18) Katilius, E.; Turanchik, T.; Lin, S.; Taguchi, A. K. W.; Woodbury, N. W. *J. Phys. Chem. B* **1999**, *103*, 7386–7389.
- (19) Kirmaier, C.; Weems, D.; Holten, D. *Biochemistry* **1999**, *38*, 11516–11530.
- (20) Roberts, J. A.; Holten, D.; Kirmaier, C. *J. Phys. Chem. B* **2001**, *105*, 5575–5584.
- (21) Laible, P. D.; Kirmaier, C.; Holten, D.; Tiede, D. M.; Schiffer, M.; Hanson, D. K. Formation of $P^+Q_B^-$ via B-branch electron transfer in mutant reaction centers. In *Photosynthesis: Mechanisms and Effects*; Garab, G., Ed.; Kluwer Academic Publishers: The Netherlands, 1998; Vol. 2, pp 849–852.
- (22) Arlt, T.; Schmidt, S.; Kaiser, W.; Lauterwasser, C.; Meyer, M.; Scheer, H.; Zinth, W. *Proc. Natl. Acad. Sci. U.S.A.* **1993**, *90*, 11757–11761.
- (23) Holzwarth, A. R.; Müller, M. G. *Biochemistry* **1996**, *35*, 11820–11831.
- (24) Nowak, F. R.; Kennis, J. T. M.; Franken, E. M.; Shkurupatov, A. Y.; Yakovlev, A.; Gast, P.; Hoff, A. J.; Aartsma, T. J.; Shuvalov, V. A. The energy level of $P^+B_A^-$ in plant pheophytin-exchanged bacterial reaction centers probed by the temperature dependence of delayed fluorescence. In *Photosynthesis: Mechanisms and Effects*; Garab, G., Ed.; Kluwer Academic Publishers: The Netherlands, 1998; Vol. 2, pp 783–786.
- (25) Parson, W. W.; Chu, Z.-T.; Warshel, A. *Biochim. Biophys. Acta* **1990**, *1017*, 251–272.
- (26) Lin, S.; Jackson, J. A.; Taguchi, A. K. W.; Woodbury, N. W. *J. Phys. Chem. B* **1999**, *103*, 4757–4763.
- (27) Goldsmith, J. O.; Boxer, S. G. *Biochim. Biophys. Acta* **1996**, *1276*, 171–175.
- (28) Alia; Matysik, J.; Erkelens, C.; Hulsbergen, F. B.; Gast, P.; Lugtenburg, J.; de Groot, H. J. M. *Chem. Phys. Lett.* **2000**, *330*, 325–330.
- (29) Lin, X.; Williams, J. C.; Allen, J. P.; Mathis, P. *Biochemistry* **1994**, *33*, 13517–13523.
- (30) Gust, D.; Moore, T. A.; Luttrull, D. K.; Seely, G. R.; Bittersmann, E.; Bensasson, R. V.; Rougee, M.; Land, E. J.; De Schryver, F. C.; Van der Auweraer, M. *Photochem. Photobiol.* **1990**, *51*, 419–426.
- (31) Peloquin, J. M.; Williams, J. C.; Lin, X.; Alden, R. G.; Murchison, H. A.; Taguchi, A. K. W.; Allen, J. P.; Woodbury, N. W. *Biochemistry* **1994**, *33*, 8089–8100.
- (32) Ogrodnik, A.; Hartwich, G.; Lossau, H.; Michel-Beyerle, M. E. *Chem. Phys.* **1999**, *244*, 461–478.
- (33) Schenck, C. C.; Blankenship, R. E.; Parson, W. W. *Biochim. Biophys. Acta* **1982**, *680*, 44–59.
- (34) Woodbury, N. W. T.; Parson, W. W. *Biochim. Biophys. Acta* **1984**, *767*, 345–361.
- (35) Arata, H.; Parson, W. W. *Biochim. Biophys. Acta* **1981**, *638*, 201–209.
- (36) Fajer, J.; Brune, D. C.; Davis, M. S.; Forman, A.; Spaulding, L. D. *Proc. Natl. Acad. Sci. U.S.A.* **1975**, *72*, 4956–4960.
- (37) Watanabe, T.; Kobayashi, M. 1.11 Electrochemistry of chlorophylls. In *Chlorophylls*; Scheer, H., Ed.; CRC Press: Boca Raton, FL, 1991; pp 287–315.
- (38) Kolbasov, D.; Scherz, A. Matrix elements play a significant role in asymmetric electron transfer in bacterial reaction centers. In *Photosynthesis: Mechanisms and Effects*; Garab, G., Ed.; Kluwer Academic Publishers: The Netherlands, 1998; Vol. 2, pp 719–722.
- (39) Kolbasov, D.; Scherz, A. *J. Phys. Chem. B* **2000**, *104*, 1802–1809.